



# Inelastic acceleration ratios for nonstructural components

Juan Carlos Obando <sup>a,\*</sup>, Julián Carrillo <sup>b</sup>, Orlando Arroyo <sup>c,d</sup>

<sup>a</sup> Associate Professor, Environmental School, Universidad de Antioquia UdeA, Calle 70 No. 52 – 21, Medellín, Colombia

<sup>b</sup> Professor, Department of Civil Engineering, Universidad Militar Nueva Granada, Colombia

<sup>c</sup> Researcher, CEER Colombian Earthquake Engineering Network, Medellín, Colombia

<sup>d</sup> Civil Engineering School, Universidad Industrial de Santander, Carrera 27 Calle 9, Bucaramanga, Colombia

## ARTICLE INFO

### Keywords:

Nonstructural components  
Nonstructural elements  
Inelastic acceleration ratios  
Inelastic response  
Floor accelerations

## ABSTRACT

Non-Structural Components (NSCs) include all the elements that are part of structures but are not typically designed to resist the loads acting on the structures. In recent major earthquakes, the seismic design of NSCs has proved to be a key feature to assure suitable performance of structures. The accelerations experienced on the floors of structures are much higher than those at ground level, and therefore, NSCs located at these levels are highly susceptible to experiencing inelastic responses. However, relatively few studies have investigated the inelastic response of NSCs. Specifically, the inelastic absolute acceleration ratio (IAR) of NSCs is an important inelastic design parameter that has been the subject of little investigation. Therefore, this research aims to investigate the inelastic response of NSCs through its IARs by using seven elastic buildings of three different structural systems and three different sets of far-field seismic ground records. The inelastic response of the NSC is characterized by the yield strength reduction coefficient ( $R$ ). The results of the study were used to develop an equation for estimating the characteristic period of ground IARs. In general, the characteristic period is equal to the fundamental period of the structure for the floor IARs and floor Inelastic Displacement Ratios (IDRs). In addition, the results helped to identify that the convergence values of the IARs mainly depend on the  $R$  factor and the damping ratio of the NSC and show consistency in both the ground IARs and the floor IARs. Furthermore, the trends of the floor IDRs are more unstable and less predictable than those of the IARs. An improved equation for predicting both ground and floor IARs is also proposed.

## 1. Introduction

Non-structural components (NSCs) include mechanical and electrical equipment, partitions, and all the contents of the structure that do not play a role in the structural system. NSCs are not commonly designed to carry the loads acting on the structure [35]. However, NSCs are also subject to the inertial effects generated by earthquakes and therefore, NSCs must be designed not only to fulfil their primary function but also to adequately resist seismic effects.

Although some requirements for the seismic design of NSCs have been previously developed [15], they are relatively recent compared with the design considerations developed for structures [17]. For this reason, the design provisions of NSCs still receive relatively little attention in structural design offices. During recent major earthquakes, this has led to poor seismic performance of NSCs in many buildings, especially in hospitals and airports, where suitable performance of NSCs and continuity of operations after an earthquake are particularly

important [22]. In addition, the relatively minor attention for the seismic design of NSCs has caused most of the economic losses in recent major seismic events, which is not surprising given that NSCs represent the highest cost in most structures [32]. Mainly for these reasons, the study of the seismic behavior of NSCs has been a very active field of research in recent decades [10].

From a seismic design point of view, NSCs can be divided into two main groups: displacement sensitive and acceleration sensitive NSCs. Displacement sensitive NSCs are seismically designed to withstand the relative displacements of their anchorage points, and acceleration sensitive NSCs are designed to withstand the acceleration requirements at their anchorage points. Most NSCs are anchored at the floor level of structures where the acceleration requirements are much higher than that perceived at ground level [13,25,26,30]. A typical configuration of the acceleration-sensitive NSCs in the buildings is shown in the Fig. 1.

In addition to the high acceleration demands experienced at floor level, the frequency content of these excitations differs significantly

\* Correspondence to: Environmental School, Universidad de Antioquia UdeA, Calle 70 No. 52 – 21, Medellín, Colombia.

E-mail addresses: [jcarlos.obando@udea.edu.co](mailto:jcarlos.obando@udea.edu.co) (J.C. Obando), [julian.carrillo@unimilitar.edu.co](mailto:julian.carrillo@unimilitar.edu.co) (J. Carrillo), [orlando.arroyo@gmail.com](mailto:orlando.arroyo@gmail.com) (O. Arroyo).

<https://doi.org/10.1016/j.istruc.2024.107374>

Received 22 February 2024; Received in revised form 13 July 2024; Accepted 22 September 2024

Available online 1 October 2024

2352-0124/© 2024 The Authors. Published by Elsevier Ltd on behalf of Institution of Structural Engineers. This is an open access article under the CC BY license (<http://creativecommons.org/licenses/by/4.0/>).

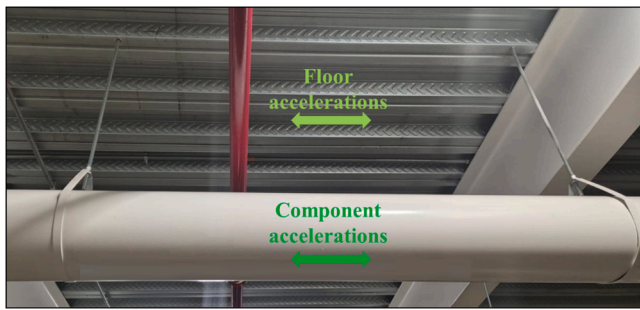


Fig. 1. Example of a typical acceleration sensitive NSC.

from the frequency content of the ground accelerations, mainly because the structures filter the ground accelerations before they reach the NSCs. These characteristics suggest that NSCs are exposed to seismic design scenarios significantly different to that of structures. Under the seismic design scenarios of NSCs, the elastic response has been extensively characterized [20,25,26,30,37]. However, and despite the high probability of developing inelastic responses, the inelastic response of NSCs has not been fully characterized.

Adam and Fotiu [2] and Azis [5] study the inelastic seismic response of NSCs anchored to inelastic structures. These structures were modelled in a simplified way as one-degree-of-freedom (DOF) oscillators, which may not adequately represent the buildings. Villaverde [36] and Chaudhuri and Villaverde [7] evaluated the inelastic seismic response of NSCs using more accurate structural models, but only consider NSC periods that coincide with the natural periods of the structure. On the other hand, Obando and López-García [27] characterized the nonlinear response of NSCs using the inelastic displacement ratio (IDR) of NSCs, that is, the ratio between the maximum inelastic and elastic displacement response of NSCs, an equation for predicting IDRs of NSCs is proposed and the main differences between IDRs of structures and IDRs of NSCs are discussed, however, only the elastic response of supporting structures is considered.

A complementary study on IDRs of NSCs has been developed by Bravo-Haro et al. [6]. These authors proposed an alternative equation to the one proposed by Obando and López-García [27] for the estimation of IDRs. Different groups of far-field and near-field seismic excitations and the nonlinear response of supporting steel structures were considered by Bravo-Haro et al. [6]. On the other hand, Anajafi et al. [4], evaluated the inelastic response of NSCs in the seismic design of the NSCs anchorages considering two elastic and inelastic supporting structural systems: special moment resisting frames (SMRF) and reinforced concrete shear walls (RCSW). The modelling of the supporting structures was carried out through multi-degree-of-freedom models and the modelling of the NSC was carried out considering the inelastic response through a bilinear hysteresis model with stiffness degradation. A similar study was developed by Magliulo and D'angela [19] considering RC structures and shaking table test protocols. However, the two previous studies do not directly compare the elastic and inelastic responses of NSCs.

Recently, Obando et al. [26] studied the inelastic response of NSCs considering the inelastic absolute acceleration ratio (IARs), that is, the ratio between the maximum inelastic and maximum elastic absolute acceleration response of the NSC. In this study, an equation is proposed to estimate the IARs, however, a single structure with a little known structural system called Thin Lightly-Reinforced Concrete Wall (TLRCW) and a single group of seismic excitations is considered, thus demonstrating the need to characterize the relationship of IARs of NSCs for a wider group of structures and seismic excitations. The IARs are important because they allow the estimation of the reduction in acceleration requirements of elastic NSCs when provided with inelastic capacity [21]. IARs are also crucial in estimating the acceleration requirements of NSCs with inherent inelastic capacity, such as air conditioners, computers, motors, instrument cabinets and piping [3].

Therefore, this research aims to study the influence of the inelastic response of NSCs on their seismic acceleration requirements by characterizing the IARs. A wide group of structures and elastic structural systems subjected to different sets of far-field seismic recordings are considered: those obtained by numerical simulation, those recommended by the Federal Emergency Management Agency [12] for cortical surface seismic zones and those recommended for subduction zones in the study of Estrella et al. [11]. Different damping ratios of the NSCs are also considered. Several prediction equations are proposed to characterize the IARs of NSCs. In all cases, the dynamic interaction of the NSCs with the structure is negligible.

## 2. Modeling and analysis of IARs

It has been observed that the characteristics of the groups of seismic record do not have a significant influence on the IDRs of NES [6], and since the IARs have a more stable and predictable behavior than the IDRs [26], this study prioritized groups of far-field seismic records. These records are commonly used to evaluate the performance of buildings and represent a large part of the seismic hazard of the studied structures: the first group of seismic records consists of 44 records recommended by the Federal Emergency Management Agency [12], the second group of seismic records considered is associated with subduction zones [11], and the third group of seismic records is that resulting from a numerical simulation of a random, nonstationary Gaussian zero-mean process, which is described in detail by Obando and Lopez-Garcia [27]. The absolute acceleration response spectra of the three groups of seismic records are shown in Fig. 2. This figure shows that the frequency content of the seismic records is typical of far-field earthquakes.

A total of seven buildings were investigated. Three steel buildings of 3, 9 and 20 stories developed by the SAC Phase II Project considering the seismic hazard for Los Angeles USA were analyzed. Fig. 3 shows the 3-story steel building; the other steel buildings considered have similar characteristics, full details of the steel buildings can be found in the study by Othori et al. [28]. In addition, three reinforced concrete (RC) wall structures of 5, 10 and 20 stories were considered. The characteristics of these structures are typical of traditional RC structures built in Chile [31]. Fig. 4 shows the 5-story RC wall building; the other RC wall buildings have similar characteristics, complete details of the RC wall structures are in the study of Steib, 2011. In addition, a 10-story RC wall and frame structure was considered. The characteristics of this structure are typical of the most recent structures built in South America in high seismic hazard zones. The characteristics of this structure are shown in Fig. 5, full details of this structure can be found in the study of Goldschmidt [14].

The north-south perimeter frames were considered for modeling the steel buildings. These steel moment resisting frames are the lateral resisting system along the north-south direction. All lateral load resisting planes along one of the principal directions are considered in the models of the RC buildings. The effective stiffnesses of the elements were used, as recommended by Paulay and Priestley [29], and rigid diaphragms were incorporated at each floor level. All buildings were modeled as 2D structures with six degrees of freedom for each element. A rigid diaphragm was considered at each floor with an equal DOF constraint to ensure uniform horizontal displacements across nodes at the same level. Lateral displacements were considered as the only degree of freedom (DOF) and the corresponding condensed stiffness matrices were obtained through static condensation techniques. The mass matrices were therefore configured as diagonal matrices whose elements are equal to the seismic masses associated with each story. The damping matrices were obtained following the Wilson-Pensien procedures [29]. The modal damping of the steel and RC buildings was set to 2% and 5%, respectively. In all models, the buildings were assumed to have linear elastic behavior. The natural periods of vibration of the buildings, as well as the nomenclature used are shown in Table 1.

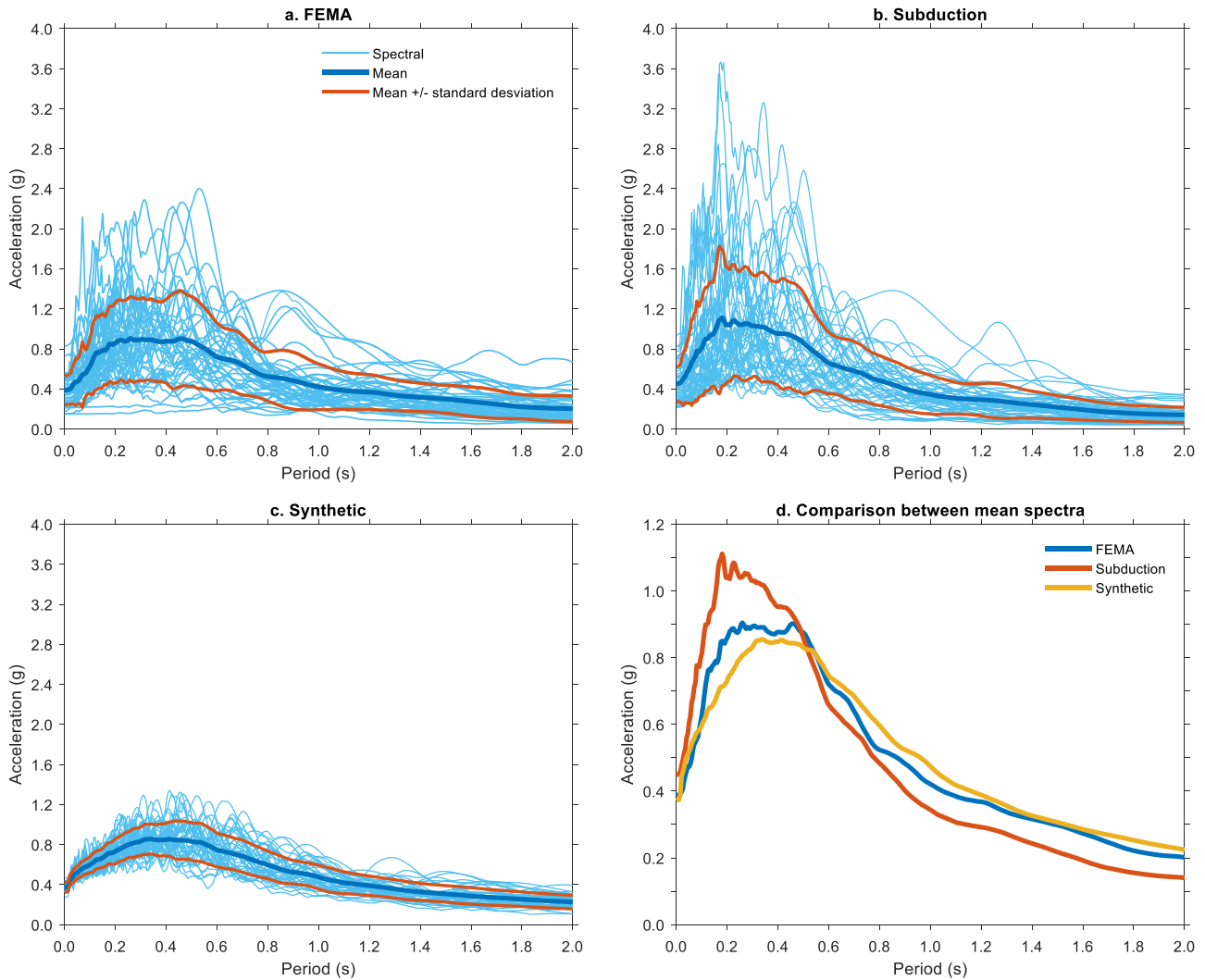


Fig. 2. Absolute acceleration response spectra of the three groups of seismic records considered.

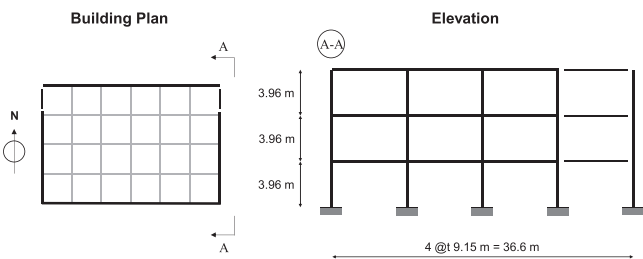


Fig. 3. Description of the 3-story steel building [28].

Although earthquake-resistant structures are typically intended to have inelastic behavior, the models used in this study assumed elastic behavior for two reasons. First, empirical evidence suggests that most structures designed according to existing codes can withstand the design earthquake without significant structural damage [9,16,22,34,33]. Second, the seismic behavior of NSCs is more relevant in essentially undamaged buildings, since the functionality after an earthquake depends on the level of damage in the NSCs [27]. This observation is particularly true for critical facilities, such as hospitals, which are designed with higher seismic requirements and are less likely to suffer structural damage. Therefore, this paper focuses on what is considered a priority, but it is expected that the observations made in this study

remain largely valid for inelastic structures, such as those structures subjected to the maximum considered earthquake (MCE).

The NSCs were modeled as one degree of freedom (DOF) system for various periods, while the nonlinear response of the NSCs was modeled with a one DOF system with a perfectly elastoplastic behavior defined by various yield-strength reduction factor  $R_p$ . The exact meaning of the  $R_p$  factor can be seen in Fig. 6, where  $u_0$  is the maximum displacement of the corresponding linear system (i.e., that of a DOF system defined by  $T_n$  and  $\xi$ ). Although NSCs exhibit different types of inelastic force-displacement relationships, the perfectly elastoplastic hysteretic model was chosen to compare with existing IDRs and IARs considering this force-displacement relationship. Due to the variability of the damping ratio of the NSCs [23] and to observe the influence of this parameter on the IARs, three damping ratios (0.01, 0.02 and 0.05) were considered.

### 3. Inelastic acceleration ratios (IARs)

The IARs is commonly defined using Eq. (1).

$$A_R = \frac{AA_{inelastic}}{AA_{elastic}} \tag{1}$$

where  $AA_{inelastic}$  is the maximum absolute acceleration of the inelastic NSC and  $AA_{elastic}$  is the absolute acceleration of the elastic NSC, with the elastic and inelastic NSC having the same damping ratio. The variability of the damping ratio of the inelastic NSC with respect to the elastic NSC

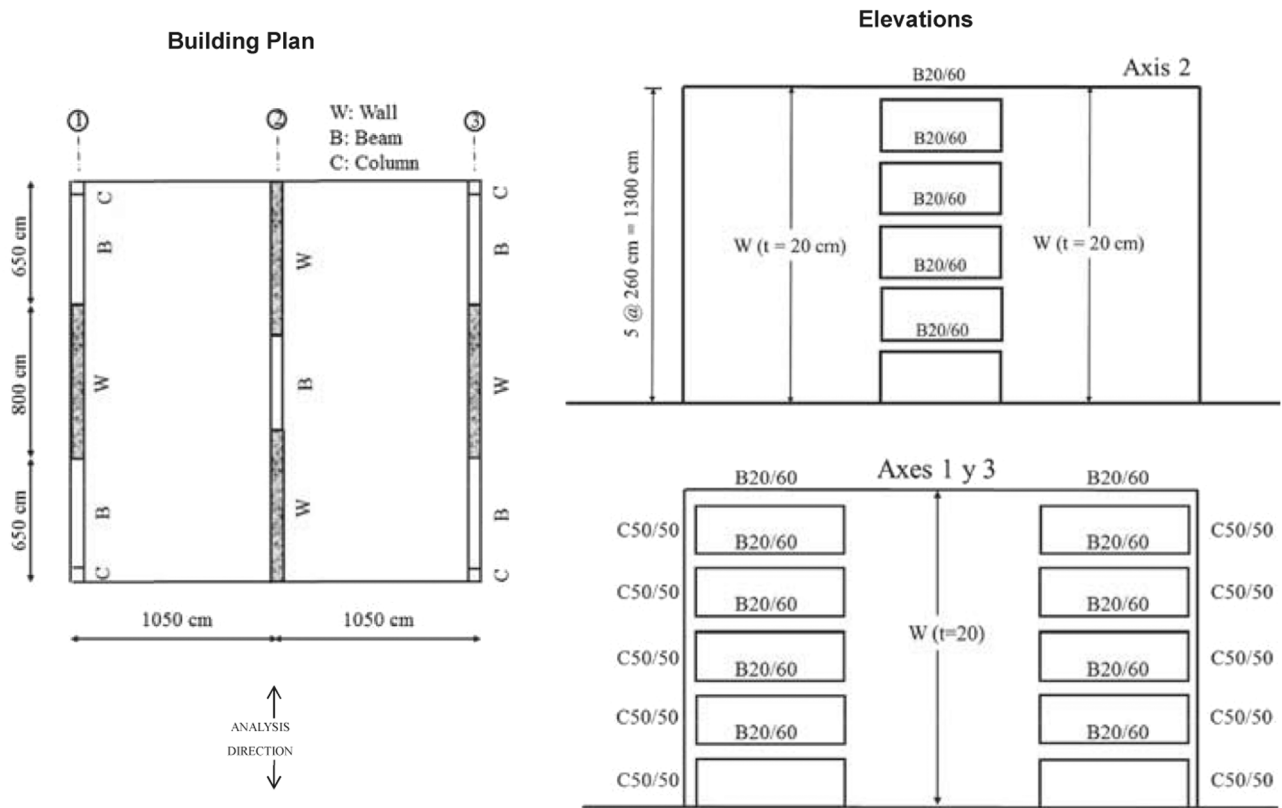


Fig. 4. Description of the 5-story RC wall building [31].

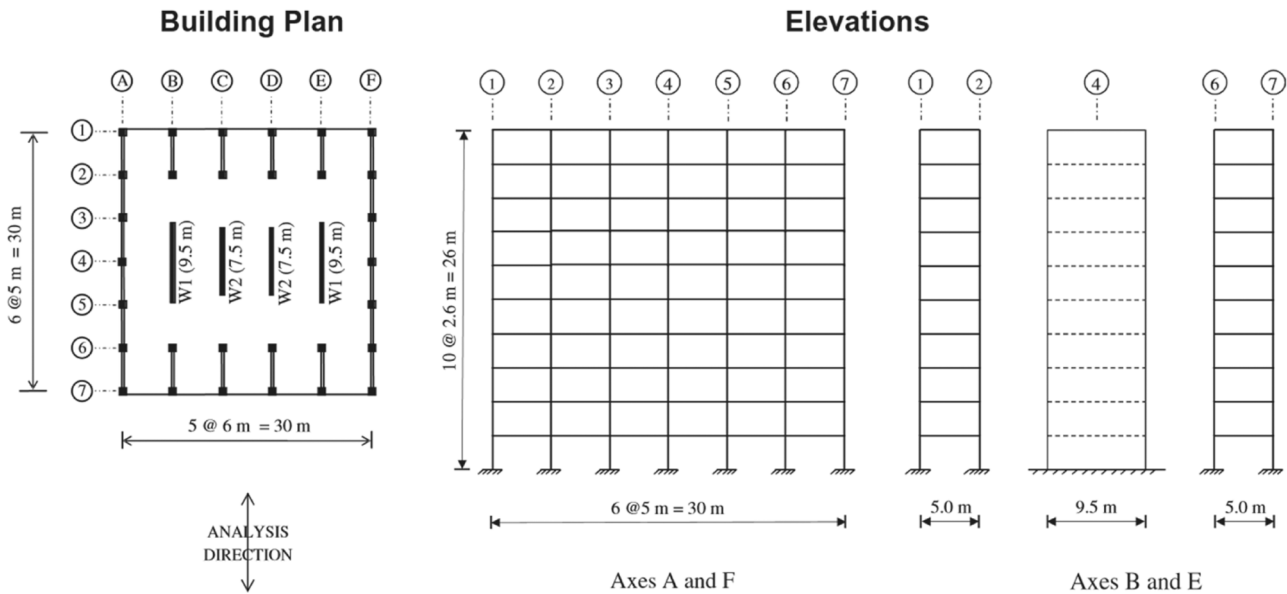


Fig. 5. Description of the 10-story RC dual wall-frame building [14].

is analyzed at the end of this study.

The IARs are initially analyzed for the case in which the damping ratio of the NSC is equal to zero. The IARs are directly equal to  $1/R_p$  where the damping is equal to zero and regardless of the input used, i.e., for any type of seismic excitation and for all periods of the NSC. This observation is explained below.

When the damping ratio of a one degree of freedom (DOF) oscillator is zero, its maximum absolute or total acceleration is determined by the Eq. (2) [8]:

$$AA_{elastic} = -\omega_n^2 |u|_{max} = \frac{f_o}{m} \quad (2)$$

where  $\omega_n$  and  $u$  are the natural frequency and the relative displacement of the oscillator, respectively, and  $f_o$  is the maximum inertial force generated by the maximum absolute acceleration of the NSC. In addition, the maximum absolute acceleration for the inelastic response also with zero damping ratio and perfect elastoplastic behavior is equal to:

**Table 1**  
Building characteristics.

Structural system	Nomenclature	Number of stories	Fundamental period T (s)	Second natural period (s)	Third natural period (s)
Steel moment-resisting frame	3S	3	0.974	0.328	0.181
	9S	9	2.098	0.800	0.469
	20S	20	3.560	1.230	0.714
RC wall	5RCW	5	0.244	0.064	0.033
	10RCW	10	0.623	0.146	0.067
	20RCW	20	1.090	0.296	0.137
Dual RC wall-frame	10RCWF	10	0.710	0.176	0.082

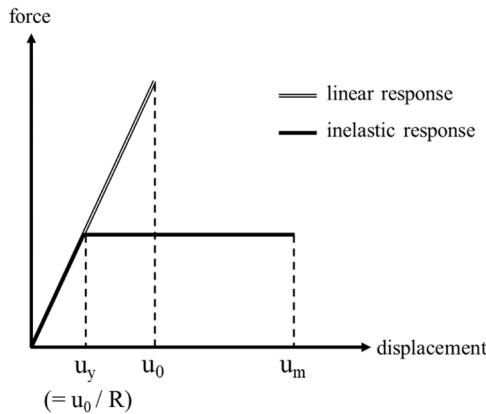


**Fig. 6.** Idealized structural response of the NSC considering the yield-strength reduction factor R.

$$AA_{inelastic} = \frac{f_o}{mR} \tag{3}$$

consequently, the inelastic ratio of absolute accelerations for the case of perfect elastoplastic behavior and damping ratio equal to zero is equal to (for any excitation and for any period of the oscillator):

$$A_R = \frac{\frac{f_o}{m}}{\frac{f_o}{mR}} \tag{4}$$

$$A_R = \frac{1}{R} \tag{5}$$

Next, the study of the IARs is developed considering different damping ratios that are commonly associated to NSCs: 1 %, 2 % and 5 % [23]. To simplify the presentation of the figures, the values considering a damping ratio equal to zero are not shown.

### 3.1. Ground IARs

Fig. 7 shows the median of the results of the ground IARs considering the three groups of seismic records: FEMA (Fig. 7a), subduction (Fig. 7c) and synthetic records (Fig. 7e). It considers two values of the NSC yield-strength reduction factor ( $R_p=4$  and 8) and three different values of damping ratio (1 %, 2 % and 5 %). In addition, a blue circle is used to mark the point on all curves where the IARs stabilize at a constant value. The period associated with these points is known as the characteristic period,  $T_c$ . The characteristic period of the IARs was defined as the period corresponding to the convergence value of the IAR plus 0.015. The value of 0.015 is the approximate minimum value that allows the establishment of a unique period  $T_p$ , values lower than 0.015 generate more than one period  $T_p$  and higher values are less precise to represent

the period of stabilization of the IARs.

Fig. 7 shows that the characteristic periods and the convergence values depend on the R factor and the damping ratio of nonstructural components. Furthermore, it shows that in the short period zone of the ground IARs, (i.e., in the zone of periods smaller than the characteristic period) the group of synthetic seismic records shows a different trend from that observed in the ground IARs of the FEMA and subduction records. This behavior is illustrated in Figs. 7b, 7d and 7f, which show the elastic and inelastic absolute acceleration response spectra for the FEMA, subduction and synthetic records, respectively. The figures consider a 5 % damping ratio. The inelastic response is shown for two  $R_p$  factors: 4 and 8.

The Figs. 7b, 7d and 7f show that the differences between the response spectra of the three groups of seismic records considered are present in the elastic response, where the synthetic records show a larger initial slope and a smaller posterior rate of change of the slope. On the other hand, the inelastic responses are similar for the three groups of seismic records. The differences in the elastic response between the synthetic records and the FEMA and subduction records produce two effects in the IARs curves of the synthetic records (Figs. 7a, 7c, 7e): a more pronounced initial negative slope and larger characteristic periods. These observations suggest that, in the short period range, the synthetic records considered are not the most appropriate for characterizing the IARs. For this reason, the results of the IARs for the group of synthetic records are not considered in the following analysis.

The characteristic periods and convergence values of the IARs for the different values of the R factor, for the different damping ratios and for the different groups of seismic records considered are presented in Table 2. The convergence values are the same for the three groups of seismic records. The Eq. (6) proposed by Obando et al. [26] can be used to estimate the convergence values for NSCs with a damping ratio of 2 %:

$$A_{Rconv} = 1 / (0.1455 + 0.8875 \cdot R_p) \tag{6}$$

where  $R_p$  is the NSC yield-strength reduction factor.

Since Eq. (6) was developed only for the NSC damping ratio of 2 %, and since the NSC damping ratio has an important influence on the convergence values of the IARs (Fig. 7), the Eq. (7) was developed throughout the nonlinear regression analysis considering different damping ratios:

$$A_{Rconv} = [ - 0.0188 + 0.0845 \xi_p + 1.01R_p - 0.0609 \xi_p R_p ]^{-1} \tag{7}$$

where  $\xi_p$  is the NSC damping ratio expressed in percentage and  $R_p$  is the NSC yield-strength reduction factor. Fig. 8a shows the convergence values of the IARs obtained using Eq. (7) versus the median of the values obtained considering FEMA and subduction records for different values of the R factor and for the three damping ratios considered in this study (1 %, 2 % and 5 %). As shown in Fig. 8a, Eq. (7) presents a good fit to the results, even considering the convergence results for the damping ratio equal to zero. Fig. 8a also shows the results of Eq. (6) for the damping ratio for which it is valid ( $\xi_p=2$  %). It can be seen in Fig. 8 that the results of Eq. (6) are similar to those obtained using Eq. (7), so either equation can be used for  $\xi_p=2$  %.

On the other hand, Fig. 7 shows the characteristic periods of the IARs. The characteristic periods (X coordinate of the light blue circles) of the IARs depend on and are proportional to the yield-strength reduction factor  $R_p$  and have an important influence of the damping ratio of the NSC. It is important to note that the characteristic period for the zero damping ratio does not exist because the IARs are equal to a single value ( $1/R_p$ ) for all NSC periods.

As shown in Fig. 7, the characteristic periods are different for each group of seismic records; however, it could be assumed conservatively for all cases that the characteristic period is equal to the larger value of the two groups of seismic records considered for the analysis (FEMA and subduction). A regression analysis helped to obtain Eq. (8) which

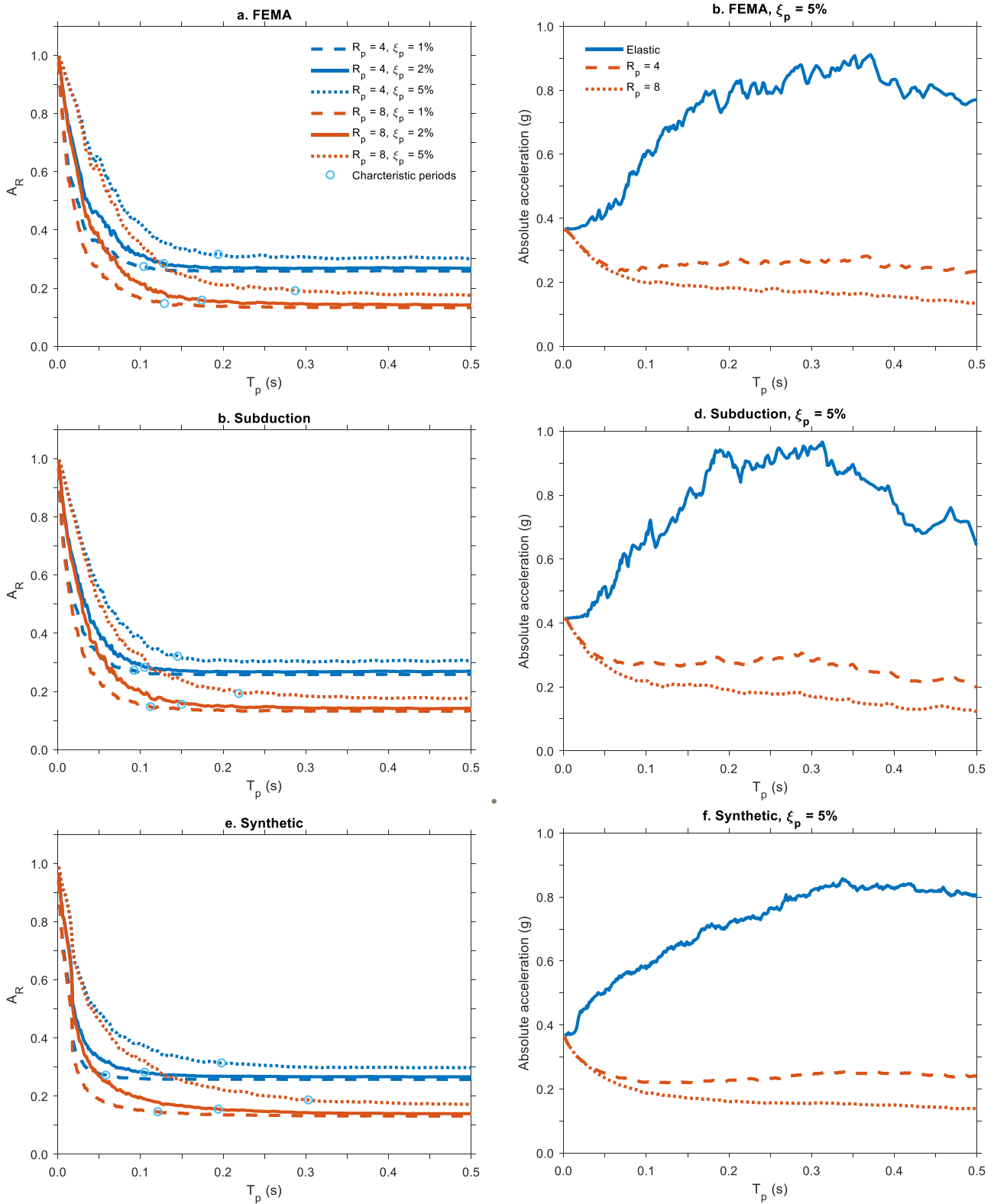


Fig. 7. Ground IARs considering different damping ratios and  $R$  factors of the NSC.

estimates the characteristic period of the IARs as a function of the  $R_p$  factor and the damping ratio of the NSC.

$$A_{R_{Tc}} = [A + BR_p + CR_p^2 + DR_p^3]^{-1} \quad (8)$$

where  $R_p$  is the yield-strength reduction factor of the NSC, and A, B, C

and D are constants presented in Table 3 that depend on the damping ratio of the NSC. Fig. 8b shows that the proposed equation has a reasonable fit to the data.

Figs. 9a, and 9c show the ground IARs for the FEMA and subduction records, respectively. The figures show long NSC periods (up to four seconds) and consider two damping ratios (1 % and 5 %) and two yield

**Table 2**  
Convergence values and characteristic periods of the ground IARs.

$R_p$	$\xi_p$ (%)	FEMA		Subduction		FEMA and Subduction	
		Convergence value	$T_c$ (s)	Convergence value	$T_c$ (s)	Mean convergence value	Max. $T_c$ (s)
2	1	0.510	0.061	0.510	0.052	0.510	0.061
	2	0.522	0.076	0.521	0.058	0.521	0.076
	5	0.557	0.091	0.555	0.075	0.556	0.091
3	1	0.342	0.089	0.341	0.068	0.342	0.089
	2	0.354	0.106	0.352	0.095	0.353	0.106
	5	0.387	0.132	0.391	0.111	0.389	0.132
4	1	0.259	0.104	0.258	0.092	0.259	0.104
	2	0.269	0.128	0.268	0.105	0.269	0.128
	5	0.301	0.194	0.306	0.145	0.304	0.194
6	1	0.175	0.117	0.174	0.101	0.174	0.117
	2	0.185	0.154	0.184	0.145	0.184	0.154
	5	0.219	0.215	0.221	0.211	0.220	0.215
8	1	0.132	0.129	0.133	0.112	0.133	0.129
	2	0.143	0.174	0.141	0.150	0.142	0.174
	5	0.176	0.287	0.178	0.219	0.177	0.287

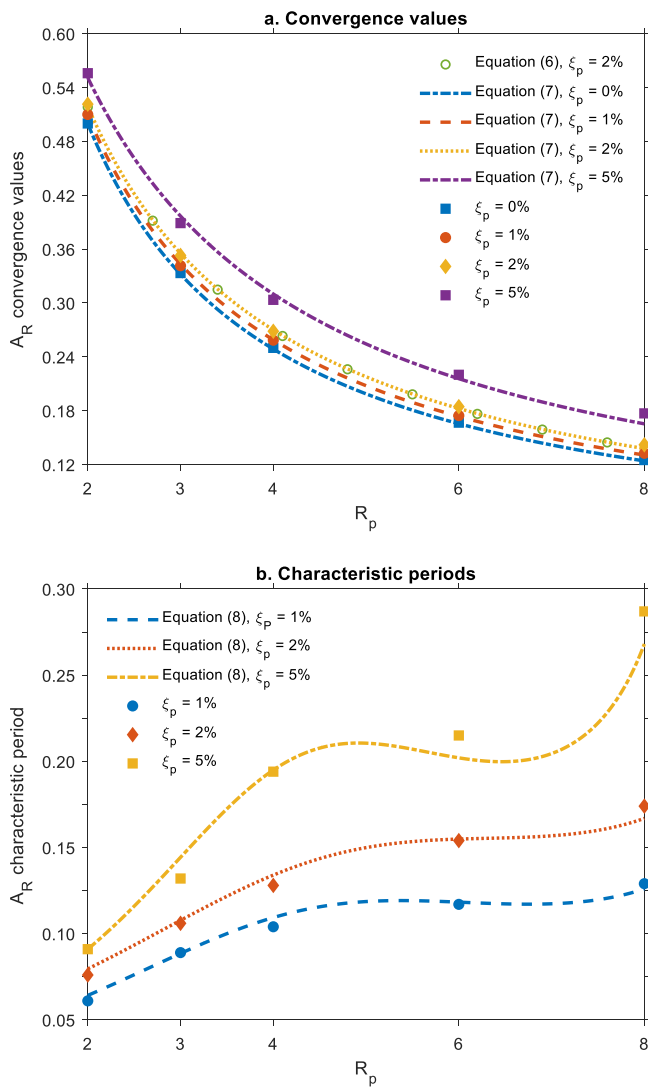


**Fig. 8.** (a) Convergence values and (b) characteristic periods of the ground IARs.

strength reduction factors  $R_p$  (2 and 6). In addition, elastic and inelastic (for  $R_p=2$ ) absolute acceleration response spectra are presented in Figs. 9b and 9d for two damping ratios of 1 % and 5 %. Although the

**Table 3**  
Values of the constants in Eq. (8).

$\xi_p$ (%)	A	B	C	D
1	33.64	-12.59	2.10	-0.12
2	25.68	-8.83	1.38	-0.07
5	29.84	-13.20	2.28	-0.13

high period zone is not so relevant because short periods are characteristics of NSCs [23], it is interesting to note in Figs. 9a, and 9c that the IARs increase slightly after about one second, i.e., once the IARs stabilize to the values that can be estimated with Eq. (7), the IARs present a slight increase from about one second. This increase is present for any value of  $R_p$  and for the two groups of seismic records.

As shown in Figs. 9b and 9d, the elastic and inelastic responses of the NSC start at the same value, but the elastic responses (dashed and solid blue lines) increase faster than the corresponding inelastic responses (dashed and solid red lines), causing the IARs to gradually decrease and stabilize at values below unity (Figs. 9a and 9c). Then, after about one second, the elastic and inelastic responses begin to converge to similar values, causing the IARs to tend toward unity (Figs. 9a and 9c) and the IARs to show a slight increase. In the Figs. 9b and 9d it can also be observed that increasing the damping ratio from 1 % to 5 % is more effective in reducing the response in the elastic spectra (blue lines) than in the inelastic spectra (red lines). For this reason, and because the IARs are the ratio between the inelastic and elastic responses, the IARs are larger for higher damping ratios than for lower damping ratios.

On the other hand, a literature review (2023) suggests that the ground IARs are assessed in a few studies [18,26]. The former studies IARs for pulsed excitations and the latter for far-fault excitations. This last work [26] proposes an equation for the estimation of the IARs; however, the variability of the NSC damping ratio is not considered. Fig. 7 shows that this parameter is important and therefore, an analysis of the IARs was performed considering different values of  $R_p$  (2, 3, 4, 6 and 8) and in turn different damping values (1 %, 2 % and 5 %). A regression analysis was used to develop Eq. (9).

$$A_R = \frac{1}{E + FR_p} + (G + He^{JR_p})e^{\left(\frac{JR_p + K}{R_p + L}\right)T_p} \quad (9)$$

where  $R_p$  is the NSC yield-strength reduction coefficient,  $T_p$  is the period of the NSC and the values of the constants E, F, G, H, I, J, K and L are presented in Table 4 as a function of the three NSC damping values considered (1 %, 2 % and 5 %). Fig. 10 shows the results of the IARs for ground accelerations for two groups of seismic excitations: FEMA and

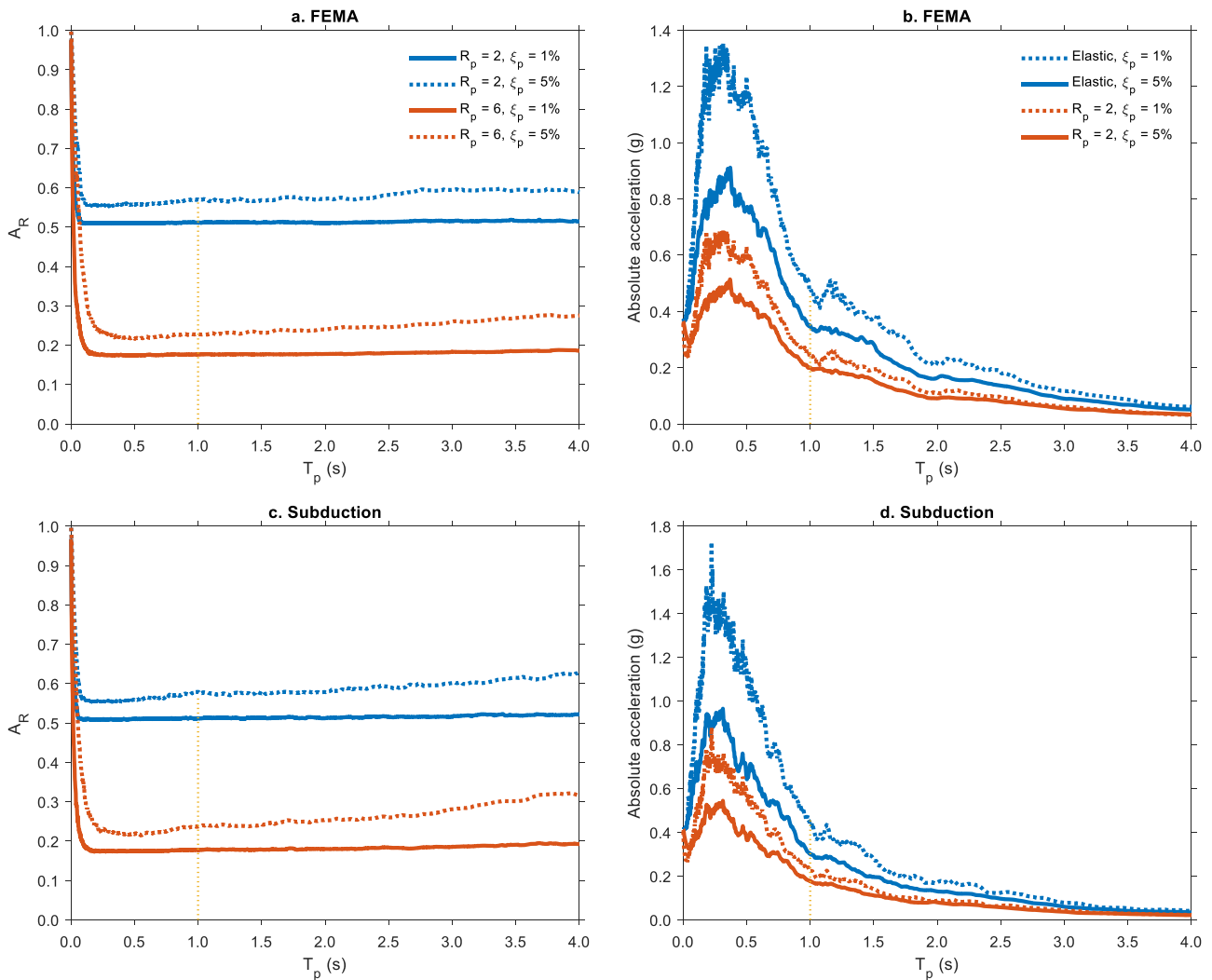


Fig. 9. Ground IARs (a, c) and elastic and inelastic absolute acceleration ground spectra (b, d) considering high NSC periods.

Table 4

Values of the constants in Eq. (9).

$\xi_p$ (%)	E	F	G	H	I	J	K	L
1	0.0542	0.9479	0.7944	-1.4334	-0.6957	-38.6990	10.6994	-0.9650
2	0.0956	0.9050	0.8363	-1.5589	-0.7160	-25.2952	4.5345	-0.9590
5	0.2350	0.7678	0.8614	-1.6893	-0.7404	-15.2297	0.9044	-0.9943

subduction compared with the results generated with Eq. (9). It considers different  $R_p$  factors for the NSC (2, 4, 6, and 8) and varying damping ratios for the NSC (1 %, 2 %, and 5 %). The Fig. 10 show that Eq. (9) generates a good estimation of the IARs.

3.2. Floor IARs

Fig. 11 shows the results of the median of the floor IDRs (Figs. 11a, 11c and 11e) and the median of the floor IARs (Figs. 11b, 11d and 11f) considering different floor accelerations and different sets of seismic records as input of the structures. To facilitate the comparison between the IDRs and the IARs, the results are presented for each relation considering the same accelerations. For all cases, the NSC yield-strength reduction factor and damping ratio is equal to three ( $R_p=3$ ) and 2 % ( $\xi_p=2\%$ ), respectively. The figures show that the floor to floor variability in the IDRs is greater than the IARs, with local minima and maxima being more pronounced and less predictable in the case of IDRs

[26]. In contrast, the IARs have more stable trends; suggesting that a predictive equation is more feasible for the floor IARs than for the floor IDRs. Fig. 11 also shows that, the characteristic period for both floor IARs and floor IDRs typically coincides with the fundamental period of the structure. For periods shorter than this characteristic period, both ratios exhibit a monotonic increase: IARs approach a value of one, while IDRs tend to infinity.

Fig. 12 shows the results of the floor IARs considering different values of the yield-strength reduction factor  $R_p$  (2, 3 and 6). The results show that the convergence of the values of the IARs as the period of the NSC increases is a function of the  $R_p$  factor and that in all cases it can be estimated by Eq. (7), i.e., the convergence values are the same for the ground and floor IARs. Fig. 12 also shows that the characteristic period of the IARs is typically equal to the fundamental period of the structure. An exception is noted for the lower floors of rigid buildings (RC wall structures, Figs. 12e and 12f), where the characteristic period can be shorter than the fundamental period of the structure.

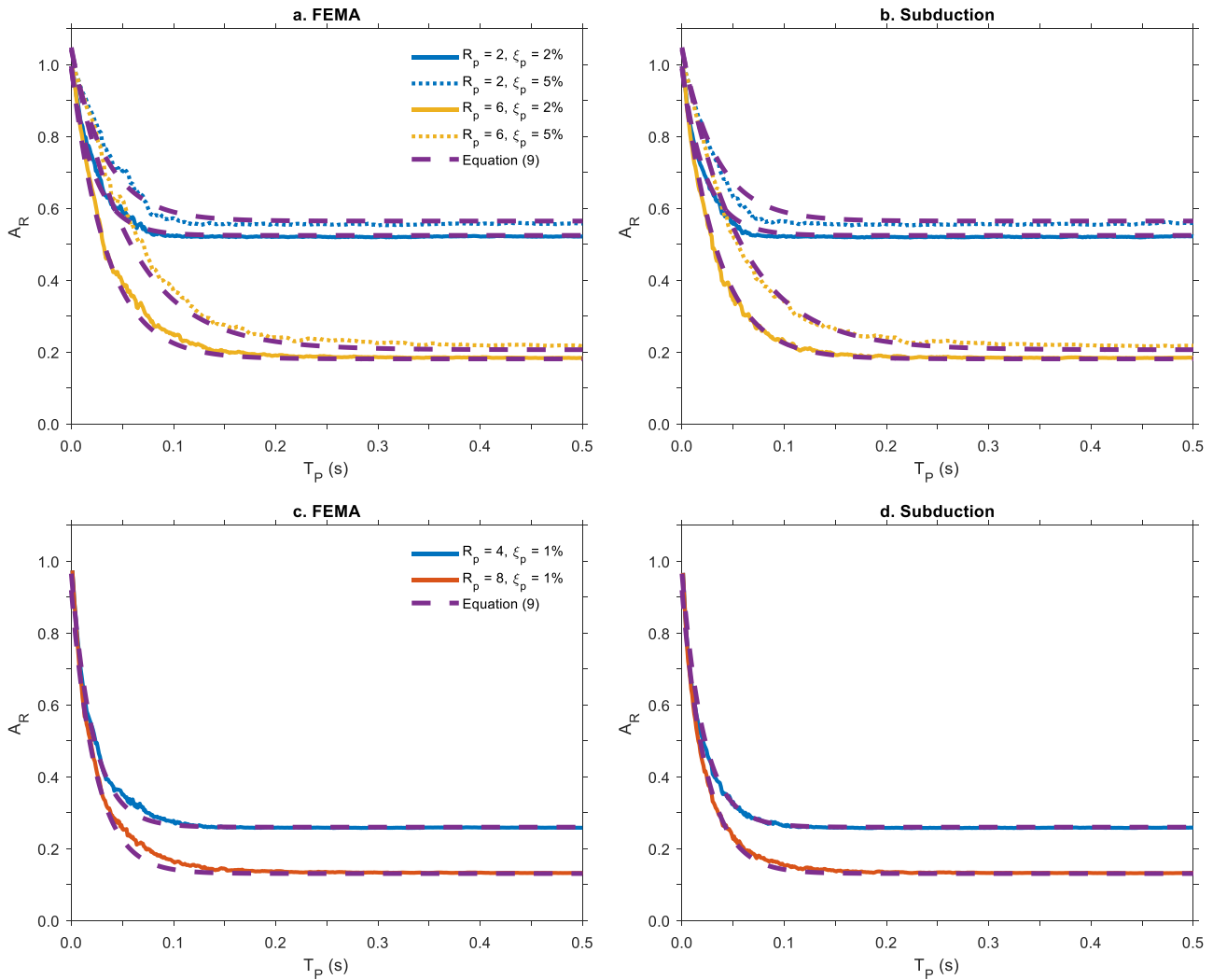


Fig. 10. Ground IARs versus Eq. (9).

To better observe this trend, the results of the first floor IARs are shown in Fig. 13. Figs. 13b, 13d, 13e, and 13f show that the characteristic period of the first floor IARs of multistory buildings is similar to that of the ground IARs, i.e., the characteristic period for these IARs can be estimated using Eq. (8). However, in the case of low-rise structures, such as the three-story steel building (3S, Fig. 13a) and the five-story RC wall structure (5RCW, Fig. 13c), the characteristic period of the first floor IARs is different from the characteristic period of the ground IARs. In the first case (3S, Fig. 13a), the characteristic period is higher than the characteristic period at ground level, while in the second case (5RCW, Fig. 13c), the characteristic period is lower than the characteristic period at ground level. Overall, the estimation of the characteristic period in the case of low-rise structures using Eq. (8) is not accurate.

On the other hand, similar to the ground IARs, Fig. 11f shows that the floor IARs initially remain stable before showing a slight increase in the high-period region of the NSC. This observation can be seen more clearly evidenced in Figs. 14a, 14c, and 14e, where the results of the floor IARs of different structures including high periods of the NSC and two damping ratios (1% and 5%) are shown. In particular, for floor IARs of structures with fundamental periods less than unity (Figs. 14a and 14c), the IARs increase slightly from periods of the NSC of approximately greater than one second. In contrast, for floor IARs of structures with fundamental periods greater than unity (Fig. 14e), the increase in IARs is shown for periods greater than the fundamental period of the structure. In addition, the increases in the IARs for large periods of the NSC are

particularly noticeable for the NSC damping ratio of 5%.

The slight increase of the IARs for high NSC periods is explained by Figs. 14b, 14d and 14f, which show the elastic and inelastic absolute acceleration response spectra for floor accelerations considering a damping ratio of 5% and considering the same floor accelerations used in Figs. 14a, 14c and 14e. It can be seen from these figures that as the period of the NSC increases, the values of the elastic and inelastic responses tend to converge to the same value. Therefore, the ratio between these responses (by definition the IARs) tends to slowly converge to one (Figs. 14a, 14c and 14e).

Although the floor and ground IARs show a slight progressive increment in the high period zone of the NSC (greater than one second), this trend is observed on unusual NSC periods. Therefore, as mentioned earlier for the ground IARs, and for practical purposes, it is reasonable to assume that the IARs converge at the initial stabilization values, i.e., just before the IARs begin to slowly increase. These initial convergence values can be estimated by Eq. (7) and depend only on the  $R_p$  factor and damping ratio of the NSC.

Given the observed similarities between ground and floor IARs, and the relatively stable trend in floor IARs, it is reasonable to apply the prediction equation for ground IARs (Eq. (9)) to estimate the floor IARs for any level within the structures. Thus, Fig. 15 compares the results obtained using Eq. (9) with the results of the floor IARs considering a constant  $R_p$  factor of 4. Similarly, Fig. 16 evaluates the results obtained using Eq. (9) for two values of the  $R_p$  factor (2 and 6) and considering

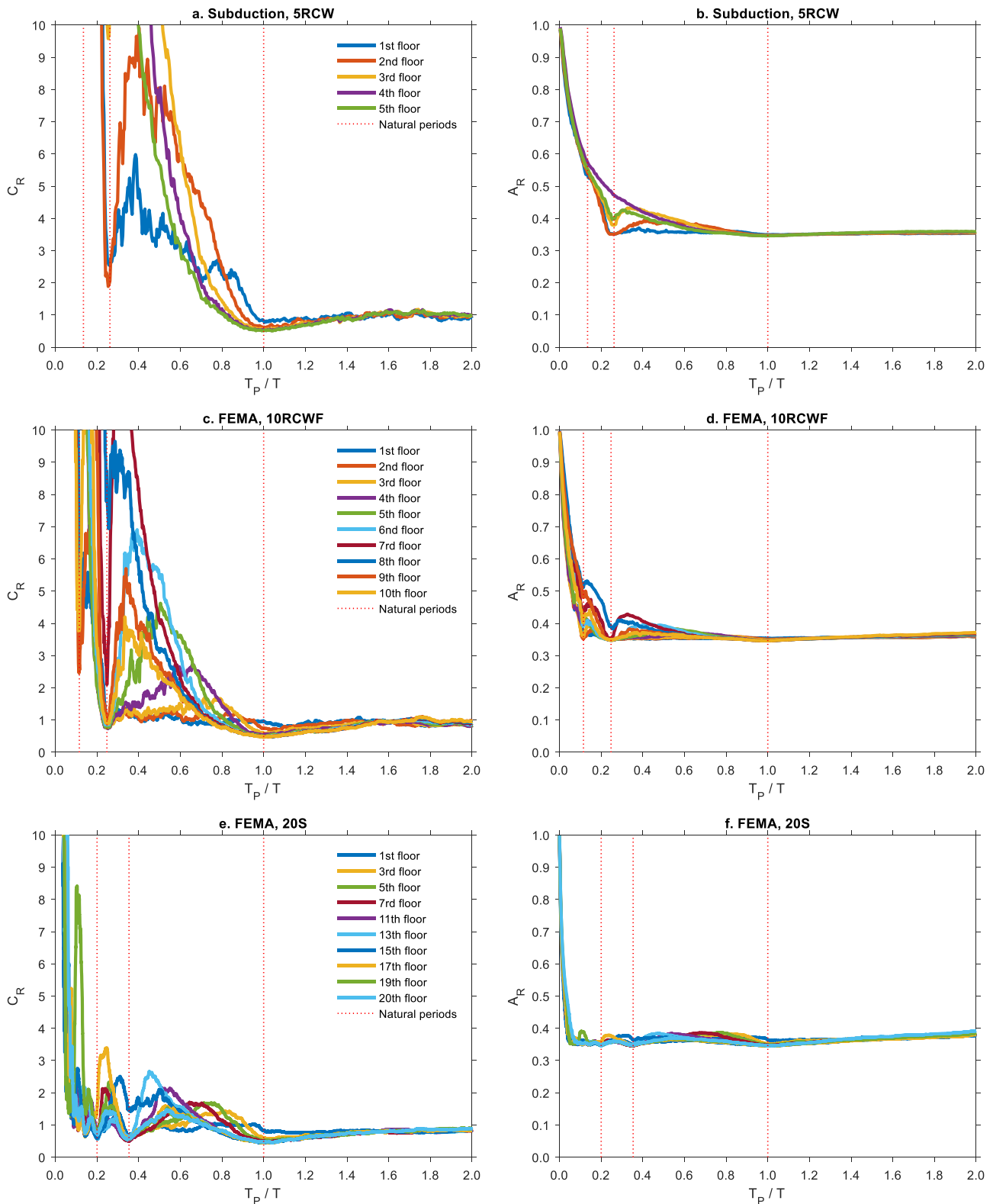


Fig. 11. Floor IDRs and IARs ( $R_p = 3, \xi_p = 2\%$ ).

two damping ratios of the NSC 1% and 5%. Although Eq. (9) was developed to estimate ground IARs, Figs. 15 and 16 show that Eq. (9) is also suitable for estimating the floor IARs for different values of both  $R_p$  factors and damping ratios of the NSC.

On the other hand, Fig. 17 shows the results of the IARs considering the variability in the damping ratios of the elastic and inelastic response

of the NSC. This relationship aids to determine the response variability of the elastic NSC when, in addition to providing inelasticity, the damping ratio of the NSC is increased from 1% to 5%. So that the IARs considering variability in the damping ratios obey the Eq. (10):

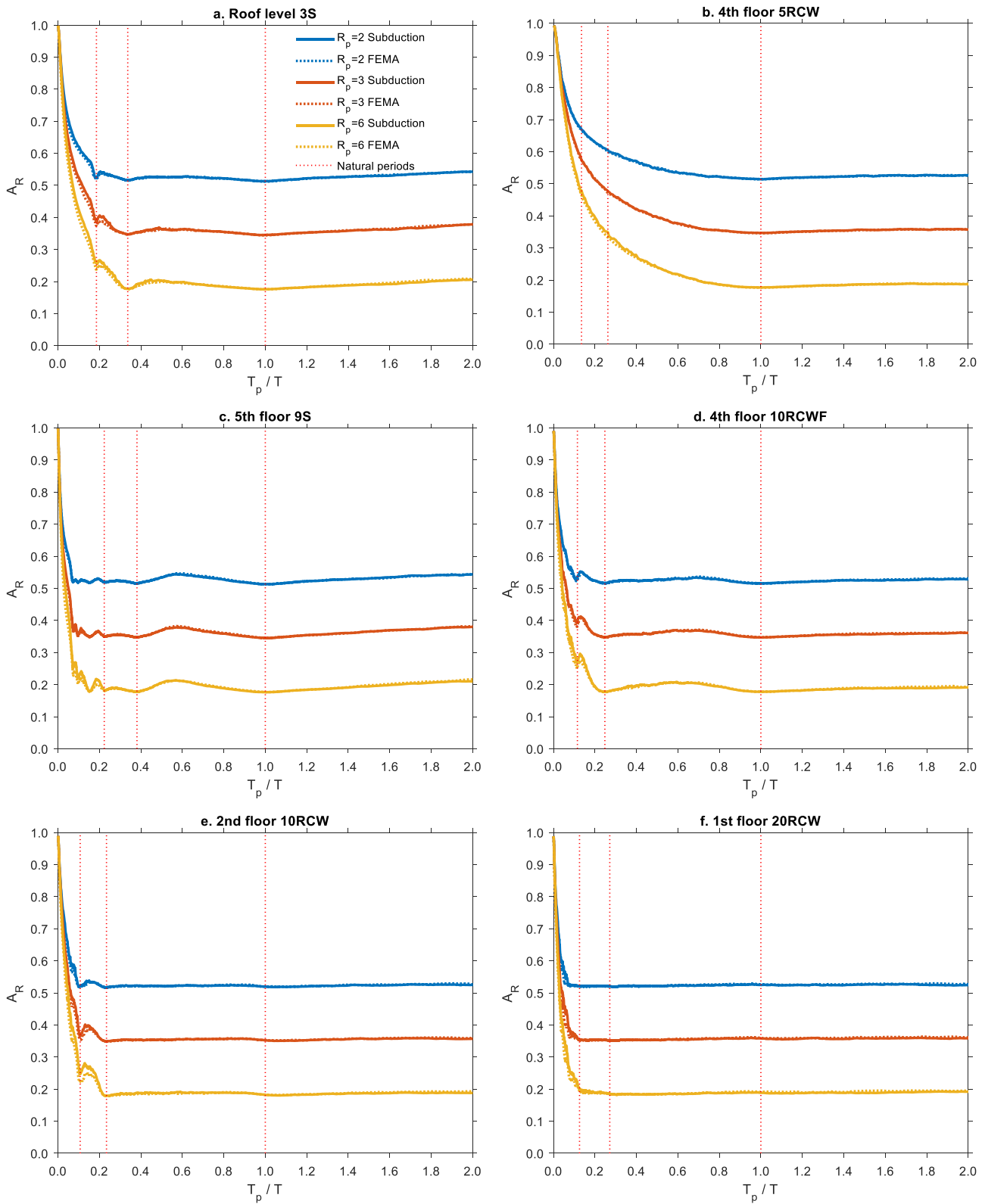


Fig. 12. Floor IARs considering different  $R_p$  factors.  $\xi_p = 2\%$ .

$$A_{R_{\xi_{var}}} = \frac{AA_{inelastic}(\xi_p=5\%)}{AA_{elastic}(\xi_p=1\%)} \quad (10)$$

where  $AA_{inelastic}(\xi_p=5\%)$  is the maximum absolute acceleration of the inelastic NSC considering a damping ratio of 5 %, and  $AA_{elastic}(\xi_p=1\%)$  is the

absolute acceleration of the corresponding elastic NSC considering a damping ratio of 1 %.

For comparison, the results of the IARs for a constant damping of 1 % are shown in the same graph. The figures show that the provision of inelasticity to the NSC is beneficial for short NSC periods, i.e., periods shorter than the characteristic period; however, in most of the cases,

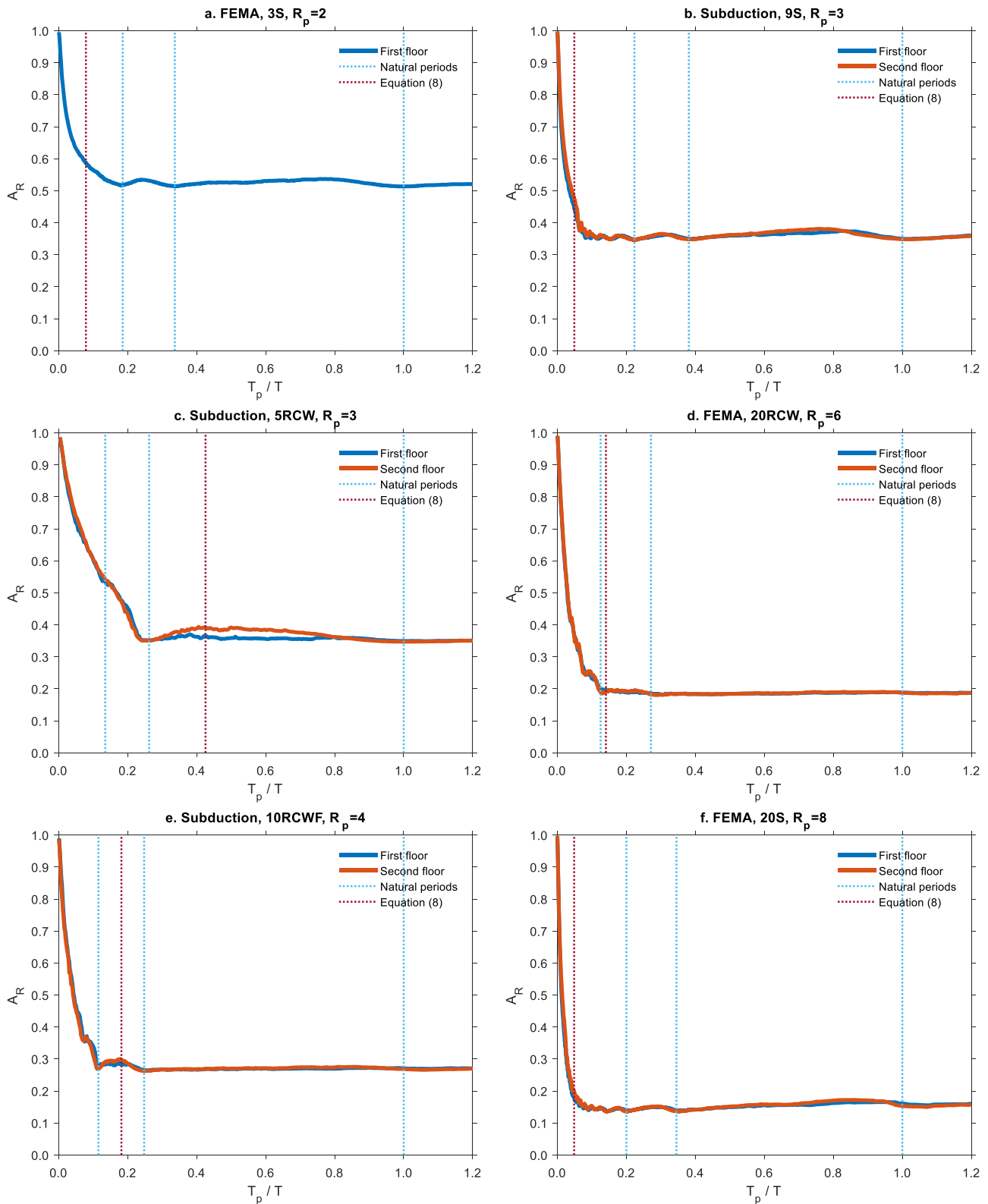


Fig. 13. First floors IARs.

further increasing the damping from 1 % to 5 % does not generate an additional decrease in the absolute acceleration response of the NSC. On the other hand, for periods longer than the characteristic period, the additional provision of damping from 1 % to 5 % is beneficial for low  $R_p$  factor values ( $R_p \leq 2$ ) and especially beneficial for periods close to the natural periods of the structure.

#### 4. Validation example

Eq. 9 of the IARs is useful for estimating the reduction in the absolute acceleration to the NSC when it is provided with inelastic capacity. An example of the application of the Eq. 9 is presented in this section. The objective is to determine how much the maximum absolute acceleration

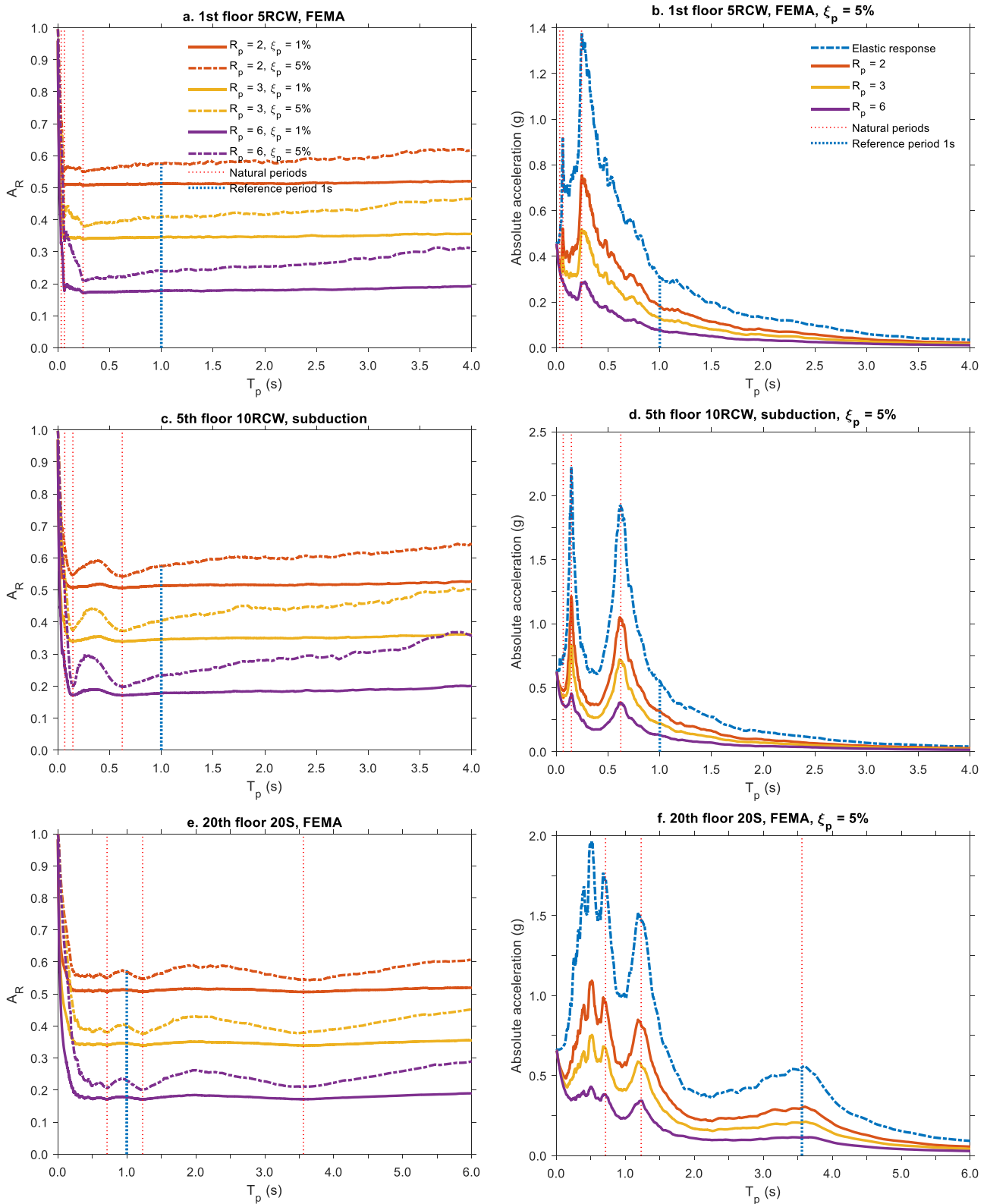


Fig. 14. Floor IARs (a, c, e) and elastic and inelastic absolute acceleration floor spectra (b, d, f) considering high NSC periods.

response of a typical elastic acceleration sensitive NSC (as the shown in the Fig. 1) is reduced, when the NSC is provided with a yield reduction strength factor of 3 ( $R_p=3$ ).

It is assumed that the NSC has a damping ratio of 2 % and is installed on the roof of a 3-story reinforced concrete moment resisting frame building. A 2D model in OpenSeesPy (3.5.1.12) was used to analyze the

building. The building is located in Cartagena, Colombia. The plan layout, the elevation drawing, and sections of the building are shown in the Fig. 18, with the blue frame indicating the selected 2D frame for the modeling of the building. The height of all floors of the building is 3.2 m. The dead load (DL) was 3 kN/m<sup>2</sup>, while the live loads (LL) for floors and roofs were set to 1.8 kN/m<sup>2</sup> and 0.5 kN/m<sup>2</sup>, respectively. The building

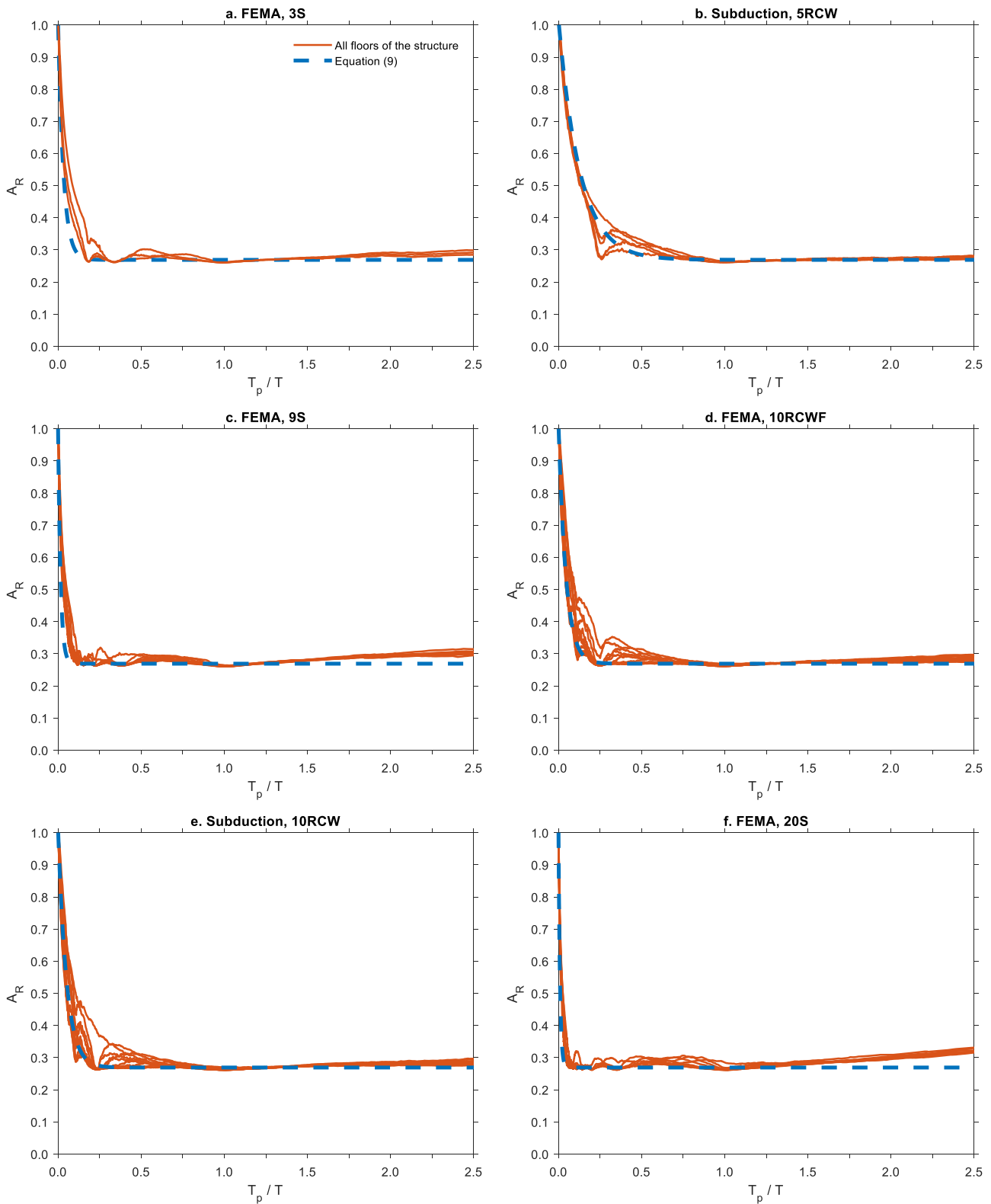


Fig. 15. Floor IARs compared with Equation (9), ( $R_p = 4$ ).

was designed in accordance with the Colombian Code for Earthquake-resistance Construction [24]. This code is similar to the ACI 318–08 [1] in its requirements for concrete frames. The building, with a fundamental period of 0.59 s, has a design spectral acceleration of  $S_a=0.40$  g. A concrete compressive strength ( $f_c$ ) of 21 MPa and an elastic Young’s modulus of steel ( $E_s$ ) of 210 GPa were used. The FEMA

records were selected to represent the seismic hazard of the zone; therefore, the building was subjected to the scaled FEMA seismic records in such a way that the response spectra is equal to the design  $S_a$  for the fundamental period of the building.

The IAR is calculated for two periods: 0.1 s and 0.3 s, so Eq. 9 is used to estimate the reduction of the absolute acceleration of the NSC for

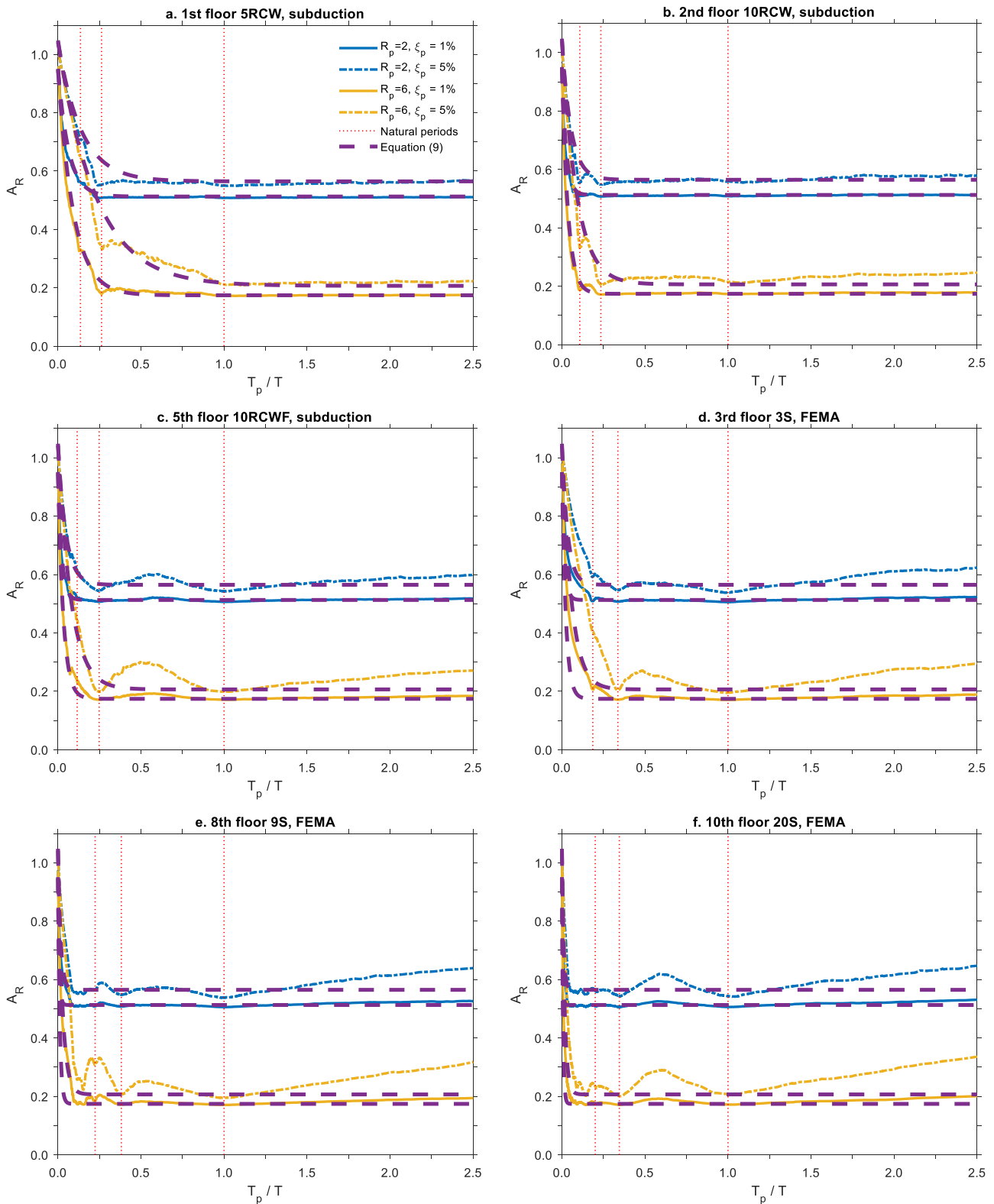


Fig. 16. Floor IARs compared with results from Eq. (9) considering different R factors and different NSCs damping ratios.

these two periods; the following two results are obtained: 0.38 and 0.36, respectively. This means that when the NSC is provided with an  $R_p$  factor of 3, the maximum absolute acceleration response is reduced by 62 % for the NSC with a period of 0.1 s and 64 % for the NSC with a period of 0.3 s. On the other hand, for the same NSC periods of 0.1 s and 0.3 s, the median simulation results are 0.47 and 0.35, respectively. Since the IARs

have a greater variation for NSC periods shorter than the characteristic period of the IARs ( $T_c$ ), Eq. 9 generates an approximate value of the IARs for the NSC period of 0.1 s and a more accurate value for the NSC period of 0.3 s.

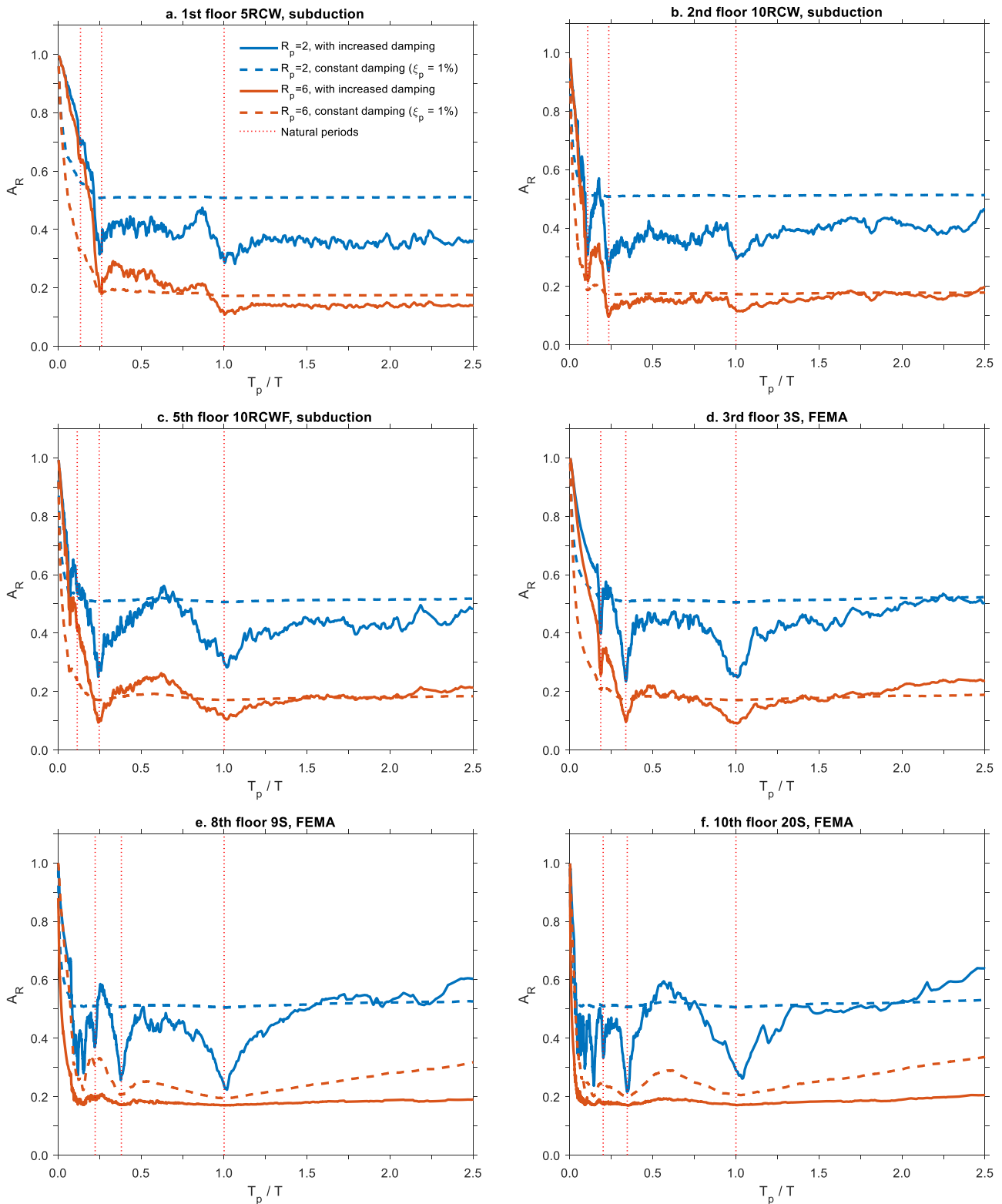


Fig. 17. IARs considering different damping ratios for the elastic and inelastic response of the NSC.

### 5. Conclusions

The study of the inelastic absolute acceleration ratios (IARs) of acceleration-sensitive nonstructural components (NSCs) was carried out considering accelerations at ground and floor levels of seven elastic buildings of three different structural systems: steel moment resisting frames, RC wall structures, RC wall and frame structures. In addition,

three groups of far-fault seismic excitations were considered as input. The main conclusions of the investigation are the following:

The convergence values of the ground and floor IARs are the same for the three groups of seismic records considered and can be estimated by Eq. (7). The convergence values depend on the damping ratio and the yield strength reduction factor coefficient  $R$  of the NSC.

The ground IARs have a characteristic period from which they

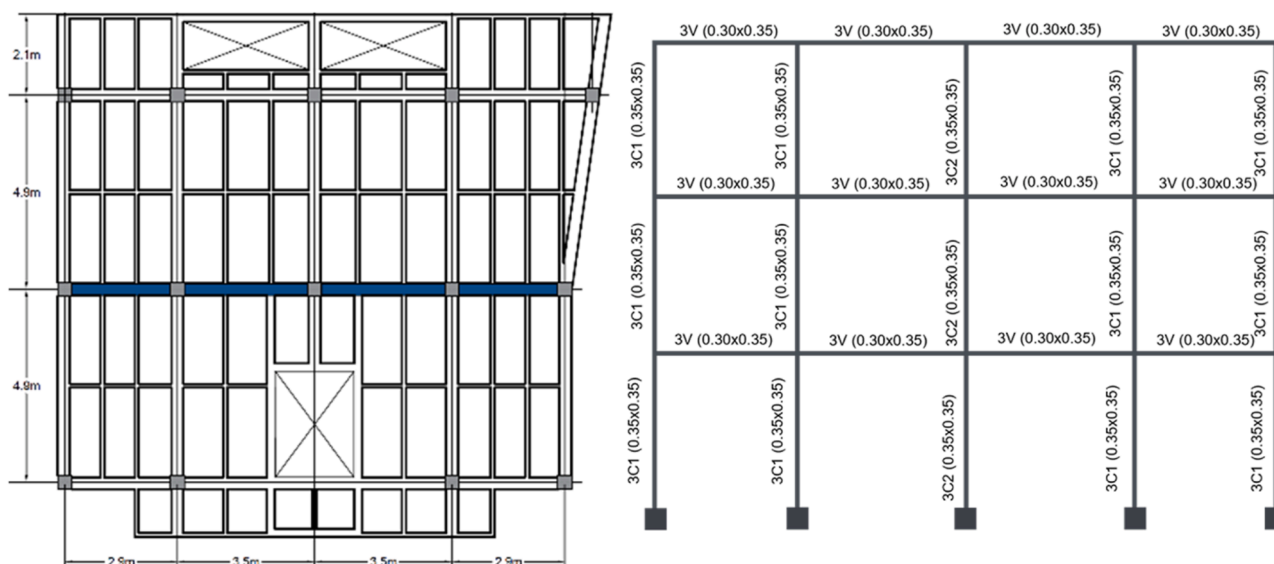


Fig. 18. Plan layout of the 3-story reinforced concrete moment resisting frame building used for the validation example.

converge to a constant value. Conservatively, the *characteristic period* of the ground IARs can be estimated with Eq. (8), which also considers the damping ratio of the NSC.

The Eq. (9) was developed for the prediction of the ground and floor IARs. The equation considers different values of the R factor and different damping ratios of the NSC (1, 2 and 5 %). The equation presents a good approximation to the results of the study.

For short periods of the NSC, the group of synthetic records presents a dissimilar trend with respect to the groups of real records, which suggests that the synthetic seismic records considered are not the most suitable for the characterization of the IARs.

The trends of the floor IDRs are more unstable and less predictable than the corresponding trends of the floor IARs. Except for the roof level, it was the reason to hinder establishing a prediction equation for floor IDRs.

Except for the IARs of the lower floors, the characteristic period, i.e., the period after which the values of the IARs or IDRs stabilize, is equal to the fundamental period of the structure for both floor IARs and floor IDRs. For lower floor accelerations, the characteristic period of the IARs is less than the fundamental period of the structure and may be less or greater than the characteristic period of the ground IARs.

Providing inelasticity to the acceleration sensitive NSCs significantly reduces their absolute acceleration requirements and further increasing the damping from 1 % to 5 % gives an additional reduction, particularly for NSCs with periods longer than the characteristic period and with low R-factors ( $R \leq 2$ ).

Recent studies [26] have shown that the inelastic response of the supporting structures does not significantly change the characteristics of the inelastic relationships of the NSCs. However, and since this study considers the essential case of elastic behavior of the supporting structures, it is recommended for future works to confirm the conclusions for structures that behave inelastically. Also, it is recommended for future works to study the characteristics of the IARs when the inelastic constitutive model of the NSCs is different from the constitutive model assumed in this paper.

#### CRedit authorship contribution statement

**Orlando Arroyo:** Data curation, Formal analysis, Funding acquisition, Resources, Software, Writing – original draft, Writing – review & editing. **Juan Carlos Obando:** Conceptualization, Formal analysis, Funding acquisition, Investigation, Methodology, Project

administration, Resources, Software, Writing – original draft, Writing – review & editing. **Julián Carrillo:** Formal analysis, Methodology, Visualization, Writing – original draft, Writing – review & editing.

#### Declaration of Competing Interest

The authors declare that they have no known competing financial interests or personal relationships that could have appeared to influence the work reported in this paper.

#### Acknowledgements

Financial support was provided by the Vicerectoría de Investigación at Universidad de Antioquia, Project No. 2022-51830 (Medellín, Colombia). This support is gratefully acknowledged.

#### References

- [1] ACI Committee, 318. Building code requirements for structural concrete (ACI 318-08) and commentary. American Concrete Institute 2008.
- [2] Adam C, Fotiu PA. Dynamic analysis of inelastic primary-secondary systems. *Eng Struct* 2000;22(1):58–71.
- [3] American Society of Civil Engineers. Minimum design loads and associated criteria for buildings and other structures. American Society of Civil Engineers; 2022.
- [4] Anajafi H, Medina RA, Santini-Bell E. Inelastic floor spectra for designing anchored acceleration-sensitive nonstructural components. *Bull Earthq Eng* 2020;18(5): 2115–47.
- [5] Aziz TS. Seismic design of secondary systems. *Adv Mitig Technol Disaster Response Lifeline Syst* 2003;637–46.
- [6] Bravo-Haro MA, Virreira JR, Elghazouli AY. Inelastic displacement ratios for non-structural components in steel framed structures under forward-directivity near-fault strong-ground motion. *Bull Earthq Eng* 2021;19(5):2185–211.
- [7] Chaudhuri SR, Villaverde R. Effect of building nonlinearity on seismic response of nonstructural components: a parametric study. *J Struct Eng* 2008;134(4):661–70.
- [8] Chopra AK. Dynamics of structures. Pearson Education India; 2007.
- [9] Clifton C, Bruneau M, MacRae G, Leon R, Fussell A. Steel structures damage from the Christchurch earthquake series of 2010 and 2011. *Bull NZ Soc Earthq Eng* 2011;44(4):297–318.
- [10] Dhakal RP, Pourali A, Tasligedik AS, Yeow T, Baird A, MacRae G, et al. Seismic performance of non-structural components and contents in buildings: an overview of NZ research. *Earthq Eng Vib* 2016;15(1):1–17.
- [11] Estrella X, Guindos P, Almazán JL. Ground motions for FEMA P-695 application in subduction zones. *Lat Am J Solids Struct* 2019;16:1–19. <https://doi.org/10.1590/1679-78255848>.
- [12] FEMA. Quantification of building seismic performance factors FEMA P-695; 2009.
- [13] Flores FX, Lopez-Garcia D, Charney FA. Assessment of floor accelerations in special steel moment frames. *J Constr Steel Res* 2015;106:154–65.
- [14] Goldschmidt, A.A. 2010. Aceleraciones de piso en edificios de estructuración mixta muros-marcos sometidos a excitaciones sísmicas. M.S. thesis, Department of

- Structural and Geotechnical Engineering, Pontificia Universidad Católica de Chile, Santiago, Chile (in Spanish).
- [15] Johnson TP, Dowell RK, Silva JF. A review of code seismic demands for anchorage of nonstructural components. *J Build Eng* 2016;5:249–53.
- [16] Jünemann R, de la Llera JC, Hube MA, Vásquez JA, Chacón MF. Study of the damage of reinforced concrete shear walls during the 2010 Chile earthquake. *Earthq Eng Struct Dyn* 2016;45(10):1621–41.
- [17] Kaushik HB, Rai DC, Jain SK. Code approaches to seismic design of masonry-infilled reinforced concrete frames: a state-of-the-art review. *Earthq Spectra* 2006;22(4):961–83.
- [18] Konstandakopoulou F, Hatzigeorgiou G. Constant-ductility inelastic displacement, velocity and acceleration ratios for systems subjected to simple pulses. *Soil Dyn Earthq Eng* 2020;131:106027.
- [19] Magliulo G, D'Angela D. Seismic response and capacity of inelastic acceleration-sensitive nonstructural elements subjected to building floor motions. *Earthq Eng Struct Dyn* 2024.
- [20] Medina RA, Sankaranarayanan R, Kingston KM. Floor response spectra for light components mounted on regular moment-resisting frame structures. *Eng Struct* 2006;28(14):1927–40.
- [21] Miranda E, Kazantzi A, Vamvatsikos D. New approach to the design of acceleration-sensitive non-structural elements in buildings. *16th Eur Conf Earthq Eng* 2018:18–21.
- [22] Miranda E, Mosqueda G, Retamales R, Pekcan G. Performance of nonstructural components during the 27 February 2010 Chile earthquake. *Earthq Spectra* 2012;28(1\_suppl1):453–71.
- [23] NIST, G.2018. GCR 18–917-43. Recommendations for improved seismic performance of non-structural components.
- [24] NSR-10. Colombian Code for earthquake-resistant construction; 2010.
- [25] Obando, J.C.2016. Diseño sísmico de componentes no estructurales sensibles a la aceleración en edificios de múltiples pisos (Doctoral dissertation, Pontificia Universidad Católica de Chile (Chile)).
- [26] Obando JC, Arroyo O, Lopez-García D, Carrillo J. Seismic response of acceleration-sensitive nonstructural components in a Thin Lightly-Reinforced Concrete Wall (TLRCW) mid-rise building. *Structures* 2022;45:1878–901.
- [27] Obando JC, Lopez-García D. Inelastic displacement ratios for nonstructural components subjected to floor accelerations. *J Earthq Eng* 2018;22(4):569–94.
- [28] Ohtori Y, Christenson RE, Spencer Jr BF, Dyke SJ. Benchmark control problems for seismically excited nonlinear buildings. *J Eng Mech* 2004;130(4):366–85.
- [29] Paulay, T., Priestley, M.N.1992. *Seismic design of reinforced concrete and masonry buildings*.
- [30] Singh MP, Moreschi LM, Suarez LE, Matheu EE. Seismic design forces. I: rigid nonstructural components. *J Struct Eng* 2006;132(10):1524–32.
- [31] Steib Pinto FJ. Aceleración de piso en edificios de hormigón armado estructurados en base a muros sometidos a excitaciones sísmicas. Chile: Pontificia Universidad Católica de Chile; 2011.
- [32] Taghavi, S., Miranda, M.M.2003. *Response assessment of nonstructural building elements*. Pacific Earthquake Engineering Research Center.
- [33] Ugalde D, Lopez-García D. Analysis of the seismic capacity of Chilean residential RC shear wall buildings. *J Build Eng* 2020;31:101369.
- [34] Ugalde D, Parra PF, Lopez-García D. Assessment of the seismic capacity of tall wall buildings using nonlinear finite element modeling. *Bull Earthq Eng* 2019;17:6565–89.
- [35] Villaverde R. Seismic design of secondary structures: state of the art. *J Struct Eng* 1997;123(8):1011–9.
- [36] Villaverde R. Simple method to estimate the seismic nonlinear response of nonstructural components in buildings. *Eng Struct* 2006;28(8):1209–21.
- [37] Vukobratović V, Fajfar P. A method for the direct estimation of floor acceleration spectra for elastic and inelastic MDOF structures. *Earthq Eng Struct Dyn* 2016;45(15):2495–511.